Original Research Article

Synthesis and Characterization of Barium-Iron Oxide Based Neodymium, Gadolinium and Praseodymium Doped Ceramic Materials

ABSTRACT

Neodymium, gadolinium, and praseodymium doped barium-iron oxide ceramic materials were synthesized by polymeric precursor method. No carbon contents or the moisture was observed in infrared spectra of the ceramics. Neodymium and gadolinium doped ceramics were crystallized in cubic lattice form, while praseodymium doped ceramic was formed in hexagonal lattice. Same results were observed from SEM images, Neodymium and gadolinium doped ceramics had similar morphological structures, but praseodymium doped ceramics had slightly different morphology. Neodymium and gadolinium doped ceramics consisted of grain-like structure, while praseodymium doped ceramic material consisted of both grain-like and pillar-like crystal structures.

Keywords: barium-iron oxide, ceramics, gadolinium, neodymium, polymeric precursor method, praseodymium.

1. INTRODUCTION

Barium oxide ceramics are popular materials amongst scientist. They have been studied so many years. These ceramics have several applications even on their own. They have also a wide range of uses especially when forms multiple oxide compounds with transition metal oxides. These compounds have considerably high dielectric constant, ferroelectric properties, piezoelectric properties, excellent optical properties, and high proton conductivity. Therefore, they are used as solar cells, piezoelectric materials, super conductors, and super capacitors [1].

When barium oxide forms a compound with iron oxides, resulting materials (barium-iron oxides) have ferromagnetic properties [2,3]. Iron oxide addition may also cause a decrease in transition temperature, therefore is used as stabilization agent for cubic phase [4]. Barium-iron oxides are also used as thermoelectric materials [5-7].

In this study, barium-iron oxide based ceramic materials were synthesized because of these wide application areas. Polymeric precursor method was used to synthesize the ceramic materials because of its advantages such as low cost, low production time, suitability for bulk production, and suitability for nanoceramic production [8,9]. Rare earth elements, i.e. neodymium, gadolinium, and praseodymium were doped to investigate their effects to the structure.

2. EXPERIMENTAL DETAILS

2.1 Materials

In the experiments, acetate and nitrate salts of barium, iron, praseodymium, neodymium and gadolinium were used. Barium acetate, iron(II) acetate, praseodymium(III) nitrate hexahydrate, neodymium(III) nitrate hexahydrate, and gadolinium(III) acetate hydrate were purchased from Sigma-Aldrich. Poly(vinyl alcohol) (PVA) (Mw 84 000 – 124 000 gmol-1) was used as the polymeric precursor; and was purchased from Sigma-Aldrich. De-ionized water and acetic acid were used as solvents. Acetic acid was obtained from Merck.

2.1 Sol preparation

In this study, the ceramic materials were synthesized by the polymeric precursor method. In the first step of the method, the polymeric precursor solution, i.e. poly(vinyl alcohol) solution (8%), was prepared. To prepare this solution, 8 g of the PVA powder was added to 92 g of de-ionized water. Then, this mixture was heated to 80 °C and stirred at this temperature until a homogenous solution obtained.

In order to prepare metal salts containing polymeric precursor solutions, proper amounts of metals acetate and nitrate salts were dissolved one by one in de-ionized water and acetic acid mixture. Then, the solutions were poured into the PVA solution drop by drop during vigorous stirring. Thus, metal acetate and nitrate containing PVA solutions were prepared. The samples were named as BIOC-1, BIOC-2, and BIOC-3 for neodymium, gadolinium and praseodymium doped samples, respectively.

Proper amounts of PVA powder and metal salts were given in Table 1.

Table 1. Amounts of the PVA powder and the metal acetates salts

Sol #	PVA Solution (8% w/w) (g)	Barium Acetate (g)	Iron Acetate (g)	Neodymium (III) Nitrate (g)	Gadolinium (III) Acetate (g)	Praseodymium (III) Nitrate (g)
BIOC - 1	20	1.414853	1.44526	0.890086	-	-
BIOC - 2	20	1.39925	1.429330	-	0.9159	-
BIOC - 3	20	1.95727	0.888598	-	-	1.1112

2.1 Ceramic materials preparation

After the preparation of the metal acetate and nitrate containing PVA solutions, the last step was carried out. The solutions were first dried at 80 °C in a vacuum oven until polymeric gels were obtained. Then, the gels were put into ceramic crucibles, and calcined at 1000 °C using a tubular furnace. After calcination, the crucibles were cooled down to the room temperature. Thus, the BIOC materials were obtained.

2.1 Characterization

Functional groups of the prepared ceramic (BIOC) materials were determined using Fourier Transform Infrared Spectroscopy (FTIR). The PerkinElmer Spectrum 100 Series FT-IR spectrometer with ATR (Attenuated Total Reflection) apparatus was used in these experiments. GNR APD 2000 Pro X-Ray Diffractometer (XRD) was used to determine crystal structures of the ceramic materials. Morphological structures of the synthesized ceramic materials were investigated by Scanning Electron Microscopy (SEM). Zeiss Supra 40VP SEM was used for evaluation. Used parameters in the SEM observations were as followings: 10 kV accelerating voltage, 10 mm working distance.

3. RESULTS AND DISCUSSION

Infrared spectra of the BIOC ceramic materials were taken in the range of 4000-500 cm-1 using infrared spectrometer (FTIR) with ATR apparatus. The spectra of the ceramics are given in Fig. 1. As the ceramics were calcined at 1000 °C, no water content was expected at the ceramics. Indeed, there is not any vibration band at around 3400-3200 cm-1 which can be related with hydroxyl (–OH) group in water. Because of the main structures are same in the ceramics, i.e. barium-iron oxide, there is not any significant difference observed in the vibrational spectra. In the spectra, broad bands appeared at 1425 cm-1. There are also sharp peaks located at 859 cm-1 and 691 cm-1. These bands are thought to arise due to barium oxide [10,11].

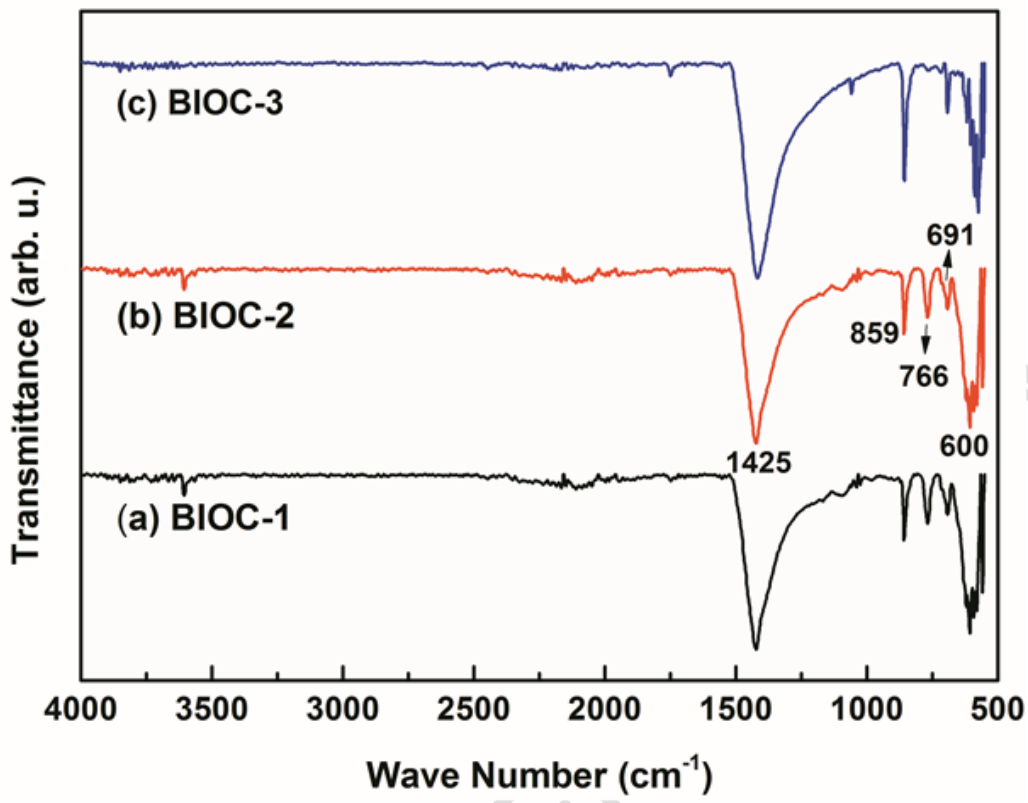

Fig. 1. FTIR spectra of the (a) BIOC-1, (b) BIOC-2, and (c) BIOC-3 ceramic materials

Crystal structures of the synthesized ceramic materials were determined using the powder X-Ray Diffractometer. XRD patterns of the BIOC materials were given in Fig. 2. Literature data showed that barium ferrite generally had a complex lattice structure (such as hexagonal, octahedral, and tetrahedral) [12-15]. Thanks to the doping of rare earth element, which acts as a stabilizer [16], this complex crystal lattice structure turned into lattice structure with single uniform and helped to increase the homogenization in the material. According to the XRD results the BIOC-1 ceramic was crystalized in c-NdBa2Fe3O7.995 structure (JCPDS number 00-050-1848). The BIOC-2 ceramic material consisted of c-GdBa2Fe3O8.17 crystal structure (JCPDS number 00-050-1841). While the BIOC-1 and the BIOC-2 ceramics were crystallized in cubic lattice form, the BIOC-3 ceramic was formed in hexagonal lattice. Crystal formula of the BIOC-3 ceramic can be shown in Fig. 2 as h-Ba6Pr2Fe4O15 (JCPDS number 01-086-1983). These results may be interpreted as the main structure of the ceramics was barium-iron oxide. However, it can be easily seen that praseodymium addition caused a change in the structure of barium-iron oxide.

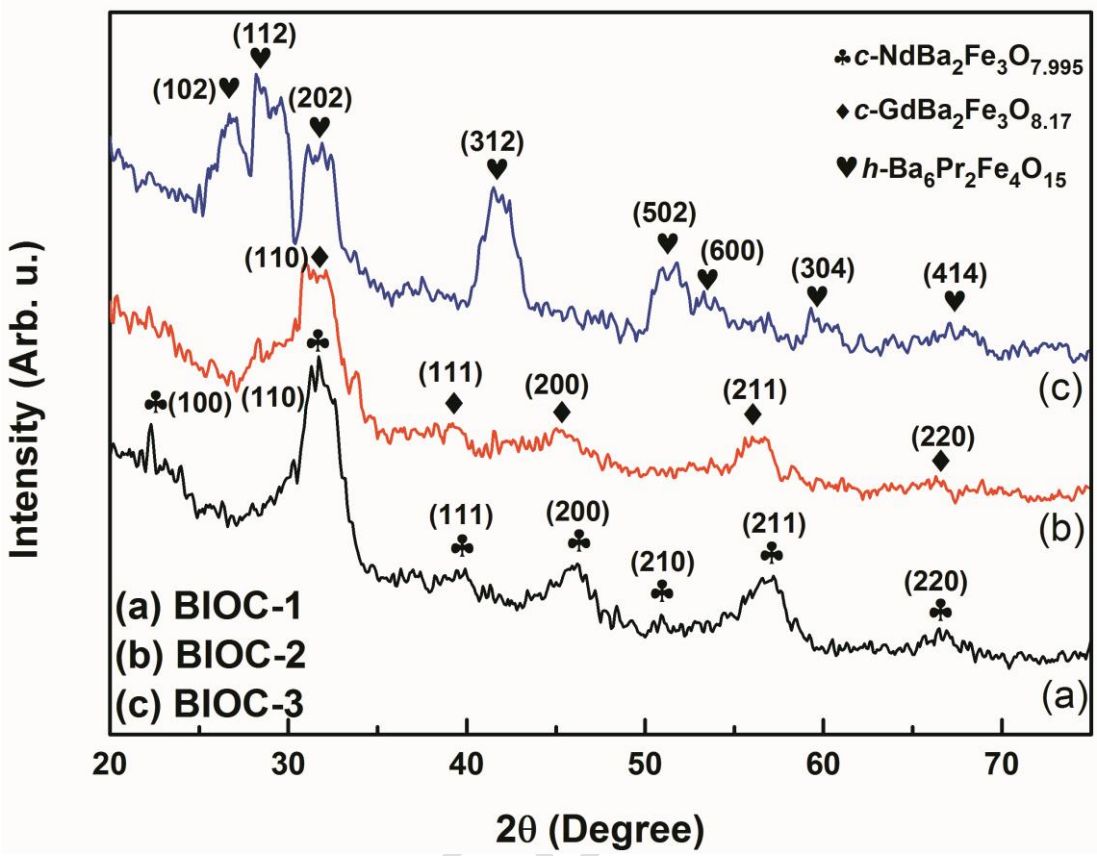

Fig. 2. XRD patterns of the (a) BIOC-1, (b) BIOC-2, and (c) BIOC-3 ceramic materials

Morphological structures of the ceramics were examined using a Field Emission Scanning Electron Microscope. SEM micrographs of the barium-iron oxide based ceramics (BIOC) can be seen in Figs. 3-5. According to the SEM images both ceramics were consisted of grain-like crystal structures. While the BIOC-1 and BIOC-2 ceramics have similar morphologic structures, the BIOC-3 ceramic has slightly different morphology (Figs. 3, 4). The BIOC-3 ceramic was consisted of both grain-like and pillar-like crystal structures (Fig. 4c). It can be easily seen from the SEM images of the ceramics taken at 40k magnification (Fig. 5) that some parts of the ceramics were agglomerated.

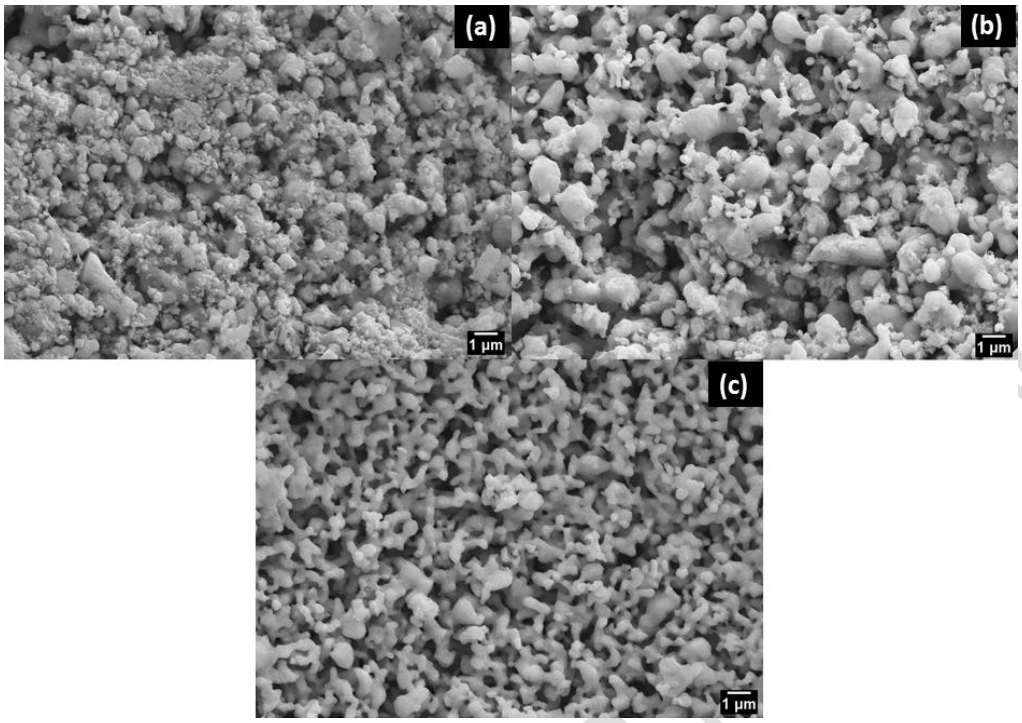

Fig. 3. SEM images of the (a) BIOC-1, (b) BIOC-2, and (c) BIOC-3 ceramic materials at 10k magnification

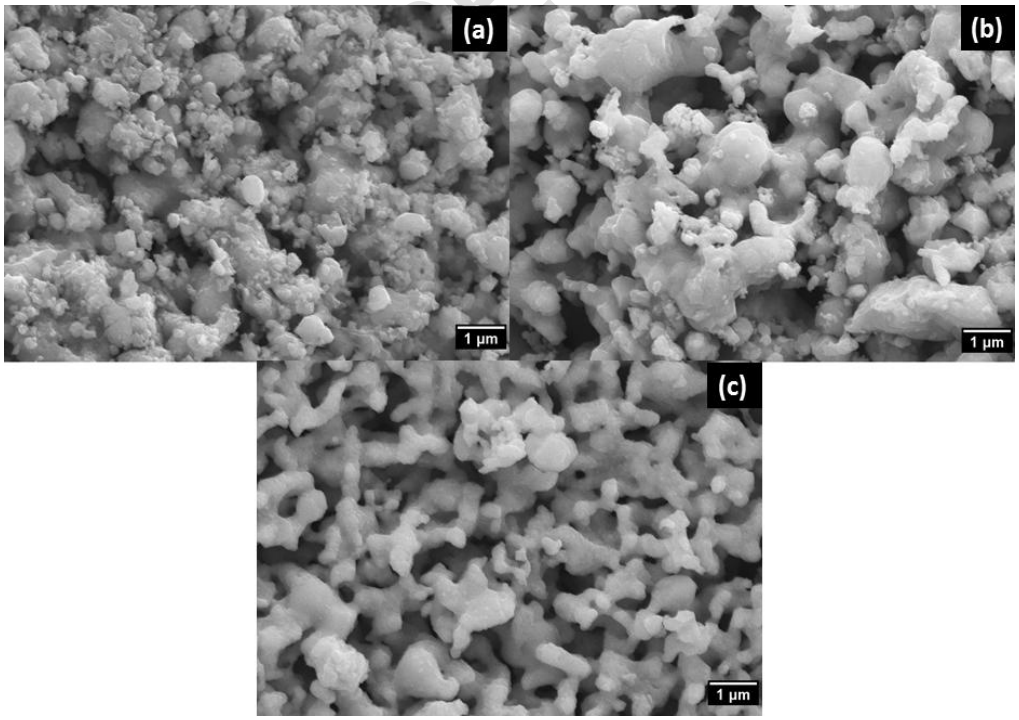

Fig. 4. SEM images of the (a) BIOC-1, (b) BIOC-2, and (c) BIOC-3 ceramic materials at 20k magnification

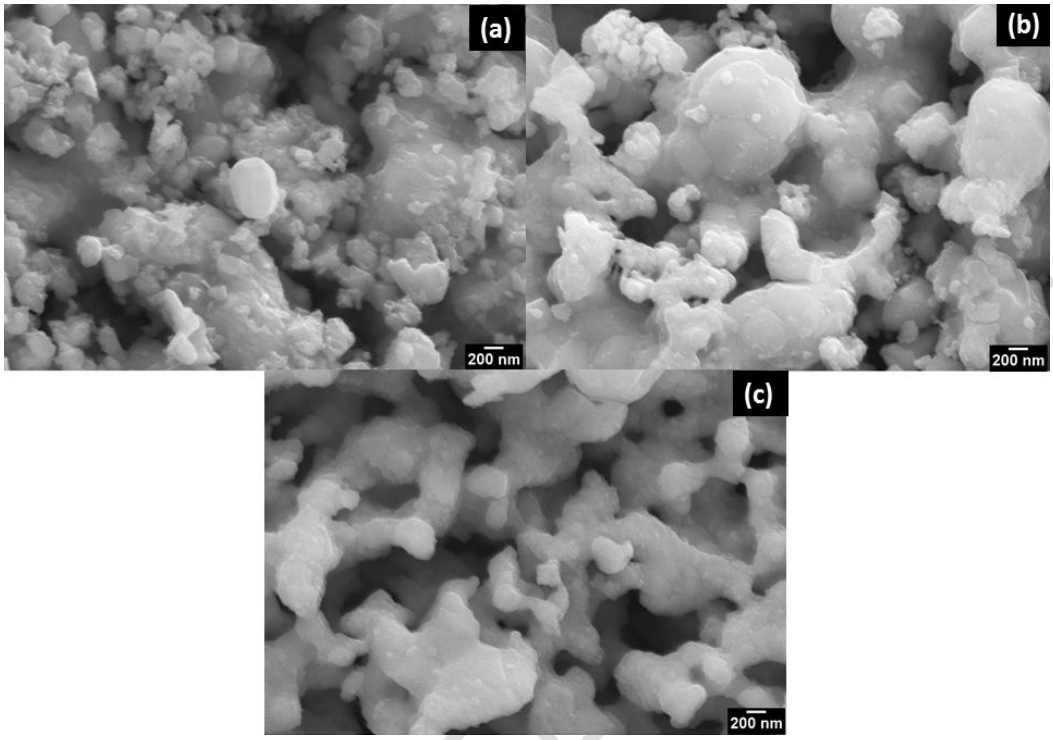

Fig. 5. SEM images of the (a) BIOC-1, (b) BIOC-2, and (c) BIOC-3 ceramic materials at 40k magnification

EDX spectra of the BIOC ceramic materials were given in Fig. 6. As seen in the figure that the ceramic materials does not contain any impurity. Elemental compositions of the ceramic materials were given in Table 2. EDX analysis results proved that the BIOC ceramic materials are mainly composed of barium-iron oxide.

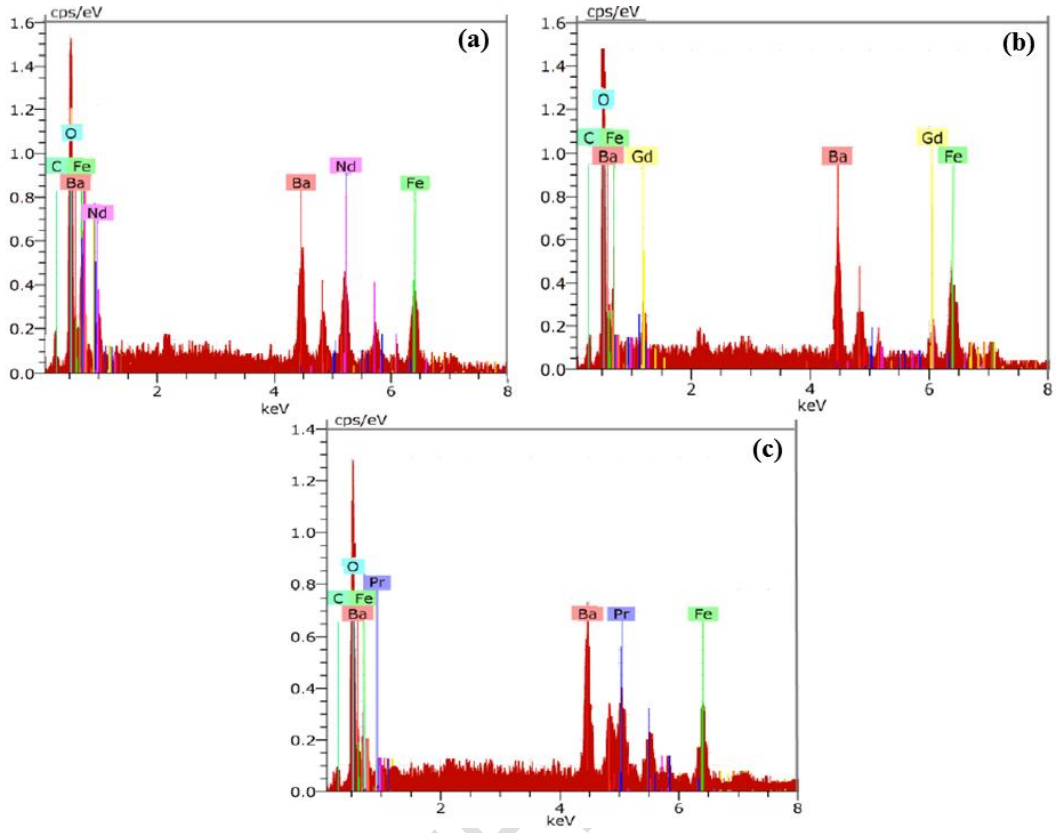

Fig. 6. EDX spectra of the (a) BIOC-1, (b) BIOC-2, and (c) BIOC-3 ceramic materials

Table 2. Elemental composition of the BIOC ceramic materials according to the EDX results

Sample	Element	Series	Composition (wt%)	Composition (at%)	Error (wt%)
BIOC-1	Barium	L-Series	30.22	11.61	1.08
	Iron	K-Series	23.30	21.99	1.02
	Neodymium	L-Series	29.61	10.82	1.13
	Oxygen	K-Series	16.87	55.58	3.11
BIOC-2	Barium	L-Series	33.17	12.40	1.28
	Iron	K-Series	30.65	28.20	1.35
	Gadolinium	L-Series	19.68	6.43	1.06
	Oxygen	K-Series	16.50	52.97	3.40
BIOC-3	Barium	L-Series	39.63	17.52	1.48
	Iron	K-Series	19.65	21.36	1.01
	Praseodymium	L-Series	27.75	11.95	1.17
	Oxygen	K-Series	12.97	49.17	2.82

4. CONCLUSION

Neodymium, gadolinium and praseodymium doped barium-iron oxide ceramic materials were produced successfully. FTIR-ATR results showed that since there was no peak between 3400-2600 cm-1, the carbon contents or the moisture was not observed in BIOC-1, BIOC-2, and BIOC-3 ceramic materials. All graphs had similar peak values and intensities. BIOC-1 and BIOC-2 ceramics were crystallized in cubic lattice form, while BIOC-3 ceramics was formed in hexagonal lattice, thanks to stabilizers such as Nd, Gd and Pr, which were rare earth elements. According to SEM images, BIOC-1 and BIOC-2 ceramics had similar morphological structures, but BIOC-3 ceramics had slightly different morphology. BIOC-1 and BIOC-2 ceramics consisted of grain-like structure, while the BIOC-3 ceramic material consisted of both grain-like and pillar-like crystal structures. It was observed that some parts of the ceramics were agglomerated. EDX analysis results proved that BIOC ceramic materials were composed of barium-iron oxide as the main material and showed that there was no impurity in the material. According to the results obtained, it is recommended to use products with especially gadolinium and neodymium additives as stabilizers in the production of a product with barium iron oxide. Praseodymium additive can also be preferred according to the desired property of the material.

COMPETING INTERESTS DISCLAIMER:

Authors have declared that no competing interests exist. The products used for this research are commonly and predominantly use products in our area of research and country. There is absolutely no conflict of interest between the authors and producers of the products because we do not intend to use these products as an avenue for any litigation but for the advancement of knowledge. Also, the research was not funded by the producing company rather it was funded by personal efforts of the authors.

REFERENCES

1. Acharya S, Torgersen J, Kim Y, Park J, Schindler P, Dadlani AL, et. al. Self-limiting atomic layer deposition of barium oxide and barium titanate thin films using a novel pyrrole based precursor. J. Mater. Chem. C. 2016;4:1945-52.

2. Kupreviciute A, Banys J, Ramoska T, Sobiestianskas R, Alawneh FMM., Gharbi N, Lupascu DC. Dielectric Properties and Conductivity of Iron Oxide-Barium Titanate Composites. Ferroelectrics. 2011;418:94-9.

3. Raveau B. Introducing Barium in, Transition Metal Oxide Frameworks: Impact upon Superconductivity, Magnetism, Multiferroism and Oxygen Diffusion and Storage. Chem. Rec. 2017;17:569-83.

4. Harizanova R, Bocker C, Avdeev G, Slavov S, Costa LC, Avramova I, Rüssel C. Microstructure and electrical conduction of iron-doped barium titanate glass-ceramics. J. Non-Cryst. Solids. 2021;560:120711.

5. Roy P, Waghmare V, Tanwar K, Maiti T. Large change in thermopower with temperature driven p–n type conduction switching in environment friendly BaxSr2xTi0.8Fe0.8Nb0.4O6 double perovskites. Phys. Chem. Chem. Phys. 2017;19:5818-29.

6. Ferreira NM, Costa FM, Kovalevsky AV, Madre MA, Torres MA, Diez JC, Sotelo A. New environmentally friendly Ba-Fe-O thermoelectric material by flexible laser floating zone processing. Scripta Mater. 2018;145:54–7.

7. Saxena M, Maiti T. Evaluation of Ba doped Sr2TiFe0.5Mo0.5O6double perovskites for high temperature thermoelectric power generation. Scripta Mater. 2018;155:85–8.

8. Aytimur A, Koçyiğit S, Temel S, Uslu I. Boron undoped and doped europium-bismuth oxide nanocomposites via the polymeric precursor technique. JOM. 2014;66:1479–84.

9. Aytimur A, Uslu I, Cinar E, Kocyigit S, Ozcan F, Akdemir A. Synthesis and characterization of boron doped bismuth–calcium–cobalt oxide nanoceramic powders via polymeric precursor technique. Ceram. Int. 2013;39:911–6.

10. Bazeeraa AZ, Amrina MI. Synthesis and Characterization of Barium Oxide Nanoparticles, IOSR JAP. 2017;1:76-80.

11. Uslu I, Cinar E, Kocyigit S, Aytimur A, Akdemir A. Fabrication and characterisation of boron doped barium stabilised bismuth cobalt oxide nanocrystalline ceramic composite. Adv. Appl. Ceram. 2013;112:336-40.

12. Šepelák V, Myndyk M, Witte R, Röder J, Menzel D, Schuster RH, Becker KD. The mechanically induced structural disorder in barium hexaferrite, BaFe 12 O 19, and its impact on magnetism. Faraday Discuss. 2014;170:121-35.

13. Mariño-Castellanos PA, Anglada-Rivera J, Cruz-Fuentes A, Lora-Serrano R. Magnetic and microstructural properties of the Ti4+-doped Barium hexaferrite. J. Magn. Magn. Mater. 2004;280:214-20.

14. Townes WD, Fang JH, Perrotta AJ. The crystal structure and refinement of ferrimagnetic barium ferrite, BaFe12O19. Z. Krist.-Cryst. Mater. 1967;25:437-49.

15. El-Sayed AH, Hemeda OM, Tawfik A, Hamad MA. Remarkable magnetic enhancement of type-M hexaferrite of barium in polystyrene polymer. AIP Adv. 2015;5:107131.

16. Zhu D, Chen YL, Miller RA. Defect clustering and nano-phase structure characterization of multi-component rare earth oxide doped zirconia-yttria thermal barrier coatings. In Ceram. Eng. Sci. Proc. 2003;24:525-34.